

Theory of light-induced resonances with collective Higgs and Leggett modes in multiband superconductors

Yuta Murotani,¹ Naoto Tsuji,² and Hideo Aoki^{1,3}

¹*Department of Physics, University of Tokyo, Hongo, Tokyo 113-0033, Japan*

²*RIKEN Center for Emergent Matter Science (CEMS), Wako 351-0198, Japan*

³*High Energy Accelerator Research Organization (KEK), Tsukuba, Ibaraki 305-0801, Japan*
(Dated: June 8, 2016)

We theoretically investigate coherent optical excitations of collective modes in two-band BCS superconductors, which accommodate two Higgs modes and one Leggett mode corresponding, respectively, to the amplitude and relative-phase oscillations of the superconducting order parameters associated with the two bands. We find, based on a mean-field analysis, that each collective mode can be resonantly excited through a nonlinear light-matter coupling when the doubled frequency of the driving field coincides with the frequency of the corresponding mode. Among the two Higgs modes, the one with higher-energy exhibits a sharp resonance with light, while the lower-energy mode has a broadened resonance width. The Leggett mode is found to be resonantly induced by a homogeneous ac electric field because the leading nonlinear effect generates a potential gradient between the two bands that couples to the relative phase of the order parameters. The resonance for the Leggett mode becomes sharper with increasing temperature. All of these light-induced collective modes along with density fluctuations contribute to the third-harmonic generation. We also predict an experimental possibility of optical detection of the Leggett mode.

PACS numbers: 74.40.Gh, 74.25.N-, 74.25.Gz, 74.70.-b

I. INTRODUCTION

Since collective modes go hand in hand with spontaneous symmetry breaking, they are one of the best probes of many-body systems. When a continuous symmetry is spontaneously broken, a massless Nambu-Goldstone (NG) mode¹⁻³ should appear in general. In the case of $U(1)$ symmetry breaking such as neutral superfluid ³He and superconductors, it takes the form of an excitation of the phase of the order parameter. In superconductors, however, electrons, being charged, are coupled to the electromagnetic field, so that the NG mode is elevated to a high energy due to the Anderson-Higgs (AH) mechanism⁴⁻⁸, making it difficult to be observed. In the vicinity of the superconducting phase transition, the massless NG mode energy can be low when the superfluid and normal components coexist and cooperatively propagate in the form of Carlson-Goldman mode^{9,10}. In addition to these, fluctuations in the amplitude of the order parameter exist¹¹ as well, and their collective excitation is called Higgs mode^{7,12,13} when the system is coupled to gauge fields. Existence of the Higgs mode in a conventional superconductor has been confirmed with Raman spectroscopy¹⁴⁻¹⁶, and more recently with terahertz (THz) spectroscopy¹⁷⁻¹⁹.

Now, if we go over to multi-component superconductors, where the superconducting order parameter consists of multiple complex components, we can expect they should accommodate versatile collective modes. Indeed, superfluid ³He is known to have multiple amplitude modes coming from spin-triplet and p -wave nature of Cooper pairs²⁰. For d -wave superconductors such as high- T_c cuprates, it has been group-theoretically shown²¹ that they can accommodate additional amplitude (Higgs)

modes coming from multiple irreducible representations of the k -dependent gap function with the D_4 point-group symmetry. As for the phase modes, multi-gap superconductors are predicted to have an out-of-phase mode between the two components of the gap function²²⁻²⁷, called “Leggett mode”.

MgB₂ is a typical example of multi-gap superconductors^{28,29}. Its double-gap structure originates from an electronic structure around the Fermi energy that comprises σ and π bands³⁰⁻³². Observation of the Leggett mode in MgB₂ has been reported with tunneling spectroscopy³³, Raman spectroscopy^{34,35} and angle-resolved photoemission spectroscopy³⁶, while no report has so far been made for the Higgs mode. A more recent family of superconductors, the iron pnictides with high T_c s, also have multi-orbital and multi-gap structures, where the electron correlation is suggested^{37,38} to bring about s_{\pm} and s_{++} pairings depending on the chemical composition and/or doping level^{39,40}. Study of collective modes in such multi-band superconductors should shed a new light on their order parameter and pairing interactions. For instance, it has been predicted that competing s - and d -wave interactions can result in different collective modes for different ground states⁴¹. Collective modes are also recently studied for systems where superconductivity coexists with diagonal orders such as spin-density wave^{42,43} or charge-density wave⁴⁴.

Multi-component superconductors thus accommodate a variety of collective modes, but we are still in need of a systematic study for them, where the Leggett and Higgs modes should be simultaneously examined by varying relative sizes of multiple superconducting gaps. This has motivated us to specifically pose a question: how are the Higgs and Leggett modes coupled to electro-

magnetic fields in multi-gap superconductors? In the single-band case, the Higgs mode couples to gauge fields nonlinearly¹⁹, which makes it possible to optically excite the mode, typically with an intense THz wave¹⁸. For multi-component superconductors we shall reveal, based on a mean-field analysis, that each collective mode can be resonantly excited through a nonlinear light-matter coupling when the doubled frequency of the driving field coincides with the frequency of each mode, as in the single-band case. The resonance itself can be interpreted as two-photon absorption by collective modes, which contrasts with Raman scattering where the energy difference between the incident and scattered photons is absorbed by elementary excitations including collective modes. We shall show that each of the two Higgs modes and the Leggett mode exhibits dramatically different sharpness in the resonance, depending on the interband pairing interaction (i.e., interband Josephson coupling) and temperature.

Second purpose of the present work is to examine how the light-induced Higgs and Leggett modes contribute to nonlinear optical responses, especially to the third-harmonic generation (THG). The resonantly induced THG at the frequency of half the superconducting gap has been observed experimentally for NbN, a single-gap superconductor¹⁸. The THG resonance is contributed from the Higgs mode¹⁹ and density fluctuations, the latter being pointed out to be dominant within the BCS mean-field theory⁴⁵. In this paper, we shall examine THG arising from the Higgs modes and density fluctuations in two-band superconductors. They are shown to have distinct resonance features, which can be utilized as an experimental probe for multi-band superconductors. We also point out another THG feature specific to multi-band cases arising from the Leggett mode, where we shall discuss the possibility of detecting the Leggett mode through THG measurement.

This paper is organized as follows. In Sec. II we construct a dynamical theory for two-band superconductivity in the BCS regime. In Sec. III we calculate the response of the relative phase to an ac electric field to derive the optical resonance of the Leggett mode. Section IV is devoted to the Higgs amplitude modes and their optical resonances. Section V examines the effects of finite temperatures on these modes. In Sec. VI we reveal how the light-induced collective modes will appear in THG. We summarize the results and future prospects in Sec. VII.

II. PSEUDOSPIN REPRESENTATION FOR TWO-BAND SUPERCONDUCTORS

Let us first derive the equation of motion for optically excited two-band superconductors, in terms of Ander-

son's pseudospins. We start with the Hamiltonian,

$$\begin{aligned} \mathcal{H} = & \sum_{\mathbf{k}\sigma} \epsilon_{\alpha}(\mathbf{k}-e\mathbf{A}(t)) \alpha_{\mathbf{k}\sigma}^{\dagger} \alpha_{\mathbf{k}\sigma} + \sum_{\mathbf{k}\sigma} \epsilon_{\beta}(\mathbf{k}-e\mathbf{A}(t)) \beta_{\mathbf{k}\sigma}^{\dagger} \beta_{\mathbf{k}\sigma} \\ & + \sum_{\mathbf{k}\mathbf{k}'} \left[V_{\alpha\alpha} \alpha_{\mathbf{k}\uparrow}^{\dagger} \alpha_{-\mathbf{k}\downarrow}^{\dagger} \alpha_{-\mathbf{k}'\downarrow} \alpha_{\mathbf{k}'\uparrow} + V_{\beta\beta} \beta_{\mathbf{k}\uparrow}^{\dagger} \beta_{-\mathbf{k}\downarrow}^{\dagger} \beta_{-\mathbf{k}'\downarrow} \beta_{\mathbf{k}'\uparrow} \right. \\ & \left. + \left(V_{\alpha\beta} \beta_{\mathbf{k}\uparrow}^{\dagger} \beta_{-\mathbf{k}\downarrow}^{\dagger} \alpha_{-\mathbf{k}'\downarrow} \alpha_{\mathbf{k}'\uparrow} + \text{h.c.} \right) \right], \end{aligned} \quad (1)$$

where subscripts α and β label the two bands, $\alpha_{\mathbf{k}\sigma}^{\dagger} (\beta_{\mathbf{k}\sigma}^{\dagger})$ creates an electron with momentum \mathbf{k} and spin σ in band $\alpha(\beta)$, $\epsilon_{\alpha\mathbf{k}}$ and $\epsilon_{\beta\mathbf{k}}$ are respective band dispersions measured from the chemical potential, $V_{\alpha\alpha}$ and $V_{\beta\beta}$ are respective intraband pairing interactions, while $V_{\alpha\beta} (= V_{\beta\alpha}^*)$ is the interband pairing interaction. $\mathbf{A}(t)$ is the vector potential representing the laser field, which is assumed to be spatially homogeneous, i.e., the superconductor is assumed to be thinner than the penetration depth and the wavelength of light. Optical interband transitions are neglected here, because we consider the incident light (such as THz waves) with energies much lower than the interband transitions. We further ignore differences in the microscopic charge distribution of Wannier orbitals between α and β bands. In this approximation, it is known that the Leggett mode at zero momentum is not affected by the Anderson-Higgs (AH) mechanism^{22-24,27}, since the interband charge transfer concomitant with the Leggett mode does not induce an electric current in real space. Hence the Leggett mode is not coupled linearly to electromagnetic fields, and survives at low energies. Even when the difference in the orbital charge distributions is taken into account, it will not contribute to the long-wavelength screening (i.e., the AH mechanism), since the interband current will only occur over typical wave vectors associated with the size of Wannier orbitals. Therefore we adopt the Hamiltonian (1) in the present paper.

Let us then define the mean fields,

$$\Psi_{\alpha\mathbf{k}} \equiv \langle \alpha_{\mathbf{k}\uparrow}^{\dagger} \alpha_{-\mathbf{k}\downarrow}^{\dagger} \rangle, \quad \Psi_{\beta\mathbf{k}} \equiv \langle \beta_{\mathbf{k}\uparrow}^{\dagger} \beta_{-\mathbf{k}\downarrow}^{\dagger} \rangle, \quad (2)$$

and

$$\begin{aligned} \Delta_{\alpha} &= -V_{\alpha\alpha} \sum_{\mathbf{k}} \Psi_{\alpha\mathbf{k}} - V_{\alpha\beta} \sum_{\mathbf{k}} \Psi_{\beta\mathbf{k}}, \\ \Delta_{\beta} &= -V_{\beta\alpha} \sum_{\mathbf{k}} \Psi_{\alpha\mathbf{k}} - V_{\beta\beta} \sum_{\mathbf{k}} \Psi_{\beta\mathbf{k}}, \end{aligned} \quad (3)$$

which yield a two-band BCS Hamiltonian,

$$\mathcal{H}_{\text{BCS}} = \mathcal{H}_{\alpha} + \mathcal{H}_{\beta}, \quad (4)$$

with

$$\begin{aligned} \mathcal{H}_{\gamma} = & \sum_{\mathbf{k}\sigma} \epsilon_{\gamma}(\mathbf{k}-e\mathbf{A}(t)) \gamma_{\mathbf{k}\sigma}^{\dagger} \gamma_{\mathbf{k}\sigma} - \Delta_{\gamma}^* \sum_{\mathbf{k}} \gamma_{\mathbf{k}\uparrow}^{\dagger} \gamma_{-\mathbf{k}\downarrow}^{\dagger} \\ & - \Delta_{\gamma} \sum_{\mathbf{k}} \gamma_{-\mathbf{k}\downarrow} \gamma_{\mathbf{k}\uparrow} + \Delta_{\gamma}^* \sum_{\mathbf{k}} \Psi_{\gamma\mathbf{k}} \end{aligned} \quad (5)$$

for $\gamma = \alpha, \beta$. Now it is convenient to introduce Anderson's pseudospin⁴⁶,

$$\boldsymbol{\sigma}_{\gamma\mathbf{k}} = \frac{1}{2}(\gamma_{\mathbf{k}\uparrow}^\dagger \quad \gamma_{-\mathbf{k}\downarrow})\boldsymbol{\tau}\begin{pmatrix} \gamma_{\mathbf{k}\uparrow}^\dagger \\ \gamma_{-\mathbf{k}\downarrow} \end{pmatrix}, \quad (6)$$

where $\boldsymbol{\tau} = (\tau^x, \tau^y, \tau^z)$ are the Pauli matrices with respect to the Nambu spinors. The Hamiltonian is then concisely expressed, up to a constant, as

$$\mathcal{H}_{\text{BCS}} = \sum_{\gamma=\alpha,\beta} \sum_{\mathbf{k}} 2\mathbf{b}_{\gamma\mathbf{k}} \cdot \boldsymbol{\sigma}_{\gamma\mathbf{k}}, \quad (7)$$

where

$$\mathbf{b}_{\gamma\mathbf{k}} = \left(-\Delta'_\gamma, -\Delta''_\gamma, \frac{\epsilon_\gamma(\mathbf{k}-e\mathbf{A}(t)) + \epsilon_\gamma(\mathbf{k}+e\mathbf{A}(t))}{2} \right) \quad (8)$$

is a pseudomagnetic field acting on the pseudospins, with Δ'_γ and Δ''_γ respectively denoting the real and imaginary parts of Δ_γ . The equation of motion for pseudospins then takes a form of the Bloch equation, $\partial\boldsymbol{\sigma}_{\gamma\mathbf{k}}/\partial t = i[\mathcal{H}_{\text{BCS}}, \boldsymbol{\sigma}_{\gamma\mathbf{k}}] = 2\mathbf{b}_{\gamma\mathbf{k}} \times \boldsymbol{\sigma}_{\gamma\mathbf{k}}$, or, for the mean fields,

$$\frac{\partial\langle\boldsymbol{\sigma}_{\gamma\mathbf{k}}\rangle}{\partial t} = 2\mathbf{b}_{\gamma\mathbf{k}} \times \langle\boldsymbol{\sigma}_{\gamma\mathbf{k}}\rangle. \quad (9)$$

We have to solve this equation to self-consistently satisfy Eq.(3), i.e.,

$$\begin{aligned} \Delta'_\gamma &= -V_{\gamma\alpha} \sum_{\mathbf{k}} \langle\sigma_{\alpha\mathbf{k}}^x\rangle - V_{\gamma\beta} \sum_{\mathbf{k}} \langle\sigma_{\beta\mathbf{k}}^x\rangle, \\ \Delta''_\gamma &= -V_{\gamma\alpha} \sum_{\mathbf{k}} \langle\sigma_{\alpha\mathbf{k}}^y\rangle - V_{\gamma\beta} \sum_{\mathbf{k}} \langle\sigma_{\beta\mathbf{k}}^y\rangle, \end{aligned} \quad (10)$$

when $V_{\alpha\beta}$ is real. We shall suppress brackets denoting the expectation values hereafter.

As the initial state we take the thermal equilibrium state, at which the free energy takes the minimum. This can be obtained through diagonalization (Bogoliubov transformation) of the mean-field Hamiltonian (4) with $\mathbf{A}(t) = 0$. With $\det V = V_{\alpha\alpha}V_{\beta\beta} - V_{\alpha\beta}V_{\beta\alpha}$, the interband coupling term in the free energy reads

$$\frac{V_{\alpha\beta}\Delta_\alpha^*\Delta_\beta + V_{\beta\alpha}\Delta_\beta^*\Delta_\alpha}{\det V}, \quad (11)$$

which is real, because $V_{\beta\alpha} = V_{\alpha\beta}^*$ due to the hermiticity of the Hamiltonian. Actually, $V_{\alpha\beta}$ can always be made real by changing the basis wave functions, so that we adopt real $V_{\alpha\beta}$ here. Equation (11) favors s_\pm pairing (which is defined as those with sign reversal, $\Delta_\alpha^*\Delta_\beta < 0$) for $V_{\alpha\beta}/\det V > 0$, while s_{++} states (with $\Delta_\alpha^*\Delta_\beta > 0$) are favored for $V_{\alpha\beta}/\det V < 0$. Here the terminology of s_\pm and s_{++} are adopted from those in iron pnictide superconductors^{37,39}. In the following, we set Δ_α and

Δ_β in the ground state to be real. Then the gap equation, which is given by the condition of the minimum free energy, becomes

$$\sigma_{\gamma\mathbf{k}}^{x,\text{eq}} = \frac{\Delta_\gamma^{\text{eq}}}{2E_{\gamma\mathbf{k}}} \tanh\left(\frac{E_{\gamma\mathbf{k}}}{2k_B T}\right), \quad \sigma_{\gamma\mathbf{k}}^{y,\text{eq}} = 0, \quad (12)$$

and the corresponding z -component is given by

$$\sigma_{\gamma\mathbf{k}}^{z,\text{eq}} = -\frac{\epsilon_{\gamma\mathbf{k}}}{2E_{\gamma\mathbf{k}}} \tanh\left(\frac{E_{\gamma\mathbf{k}}}{2k_B T}\right), \quad (13)$$

which is derived from Eqs.(9, 12) with $\partial_t\sigma_{\gamma\mathbf{k}}^y = 0$. Here the superscript “eq” denotes the equilibrium values,

$$E_{\gamma\mathbf{k}} = \sqrt{\epsilon_{\gamma\mathbf{k}}^2 + |\Delta_\gamma^{\text{eq}}|^2}, \quad (14)$$

is the quasi-particle energy in each band, k_B is the Boltzmann constant, and T is the temperature.

When the system is irradiated by a laser with weak intensity, we can linearize Eq.(9) with respect to the deviations from the equilibrium,

$$\partial_t\delta\sigma_{\gamma\mathbf{k}}^x(t) = -2\sigma_{\gamma\mathbf{k}}^{z,\text{eq}}\delta\Delta''_\gamma(t) - 2\epsilon_{\gamma\mathbf{k}}\delta\sigma_{\gamma\mathbf{k}}^y(t), \quad (15)$$

$$\begin{aligned} \partial_t\delta\sigma_{\gamma\mathbf{k}}^y(t) &= 2\epsilon_{\gamma\mathbf{k}}\delta\sigma_{\gamma\mathbf{k}}^x(t) + 2\sigma_{\gamma\mathbf{k}}^{x,\text{eq}}\delta b_{\gamma\mathbf{k}}^z(t) \\ &\quad + 2\Delta_\gamma^{\text{eq}}\delta\sigma_{\gamma\mathbf{k}}^z(t) + 2\sigma_{\gamma\mathbf{k}}^{z,\text{eq}}\delta\Delta'_\gamma(t), \end{aligned} \quad (16)$$

$$\partial_t\delta\sigma_{\gamma\mathbf{k}}^z(t) = -2\Delta_\gamma^{\text{eq}}\delta\sigma_{\gamma\mathbf{k}}^y(t) + 2\sigma_{\gamma\mathbf{k}}^{x,\text{eq}}\delta\Delta''_\gamma(t), \quad (17)$$

where we have defined the deviations, $\delta\boldsymbol{\sigma}_{\gamma\mathbf{k}}(t) = \boldsymbol{\sigma}_{\gamma\mathbf{k}}(t) - \boldsymbol{\sigma}_{\gamma\mathbf{k}}^{\text{eq}}$, $\delta\Delta'_\gamma(t) = \Delta'_\gamma(t) - \Delta_\gamma^{\text{eq}}$, $\delta\Delta''_\gamma(t) = \Delta''_\gamma(t) - 0$, and the effect of the laser, $\delta b_{\gamma\mathbf{k}}^z(t) = b_{\gamma\mathbf{k}}^z(t) - \epsilon_{\gamma\mathbf{k}} \simeq (e^2/2)\sum_{ij}(\partial_{k_i}\partial_{k_j}\epsilon_{\gamma\mathbf{k}})A_i(t)A_j(t)$. Fourier transforms, e.g. $\delta\Delta'_\gamma(t) = \int_{-\infty}^{\infty} \frac{d\omega}{2\pi} \delta\Delta'_\gamma(\omega)e^{i\omega t}$, give

$$\begin{aligned} \begin{pmatrix} \delta\sigma_{\gamma\mathbf{k}}^x(\omega) \\ \delta\sigma_{\gamma\mathbf{k}}^y(\omega) \\ \delta\sigma_{\gamma\mathbf{k}}^z(\omega) \end{pmatrix} &= - \begin{pmatrix} 4\epsilon_{\gamma\mathbf{k}}^2 & 2i\omega\epsilon_{\gamma\mathbf{k}} & 4\Delta_\gamma\epsilon_{\gamma\mathbf{k}} \\ -2i\omega\epsilon_{\gamma\mathbf{k}} & 4E_{\gamma\mathbf{k}}^2 & -2i\omega\Delta_\gamma \\ 4\Delta_\gamma\epsilon_{\gamma\mathbf{k}} & 2i\omega\Delta_\gamma & 4\Delta_\gamma^2 \end{pmatrix} \\ &\quad \times \frac{\sigma_{\gamma\mathbf{k}}^x}{\Delta_\gamma(4E_{\gamma\mathbf{k}}^2 - \omega^2)} \begin{pmatrix} -\delta\Delta'_\gamma(\omega) \\ -\delta\Delta''_\gamma(\omega) \\ \delta b_{\gamma\mathbf{k}}^z(\omega) \end{pmatrix} \end{aligned} \quad (18)$$

with shorthand $\Delta_\gamma \equiv \Delta_\gamma^{\text{eq}}$ and $\sigma_{\gamma\mathbf{k}} \equiv \sigma_{\gamma\mathbf{k}}^{\text{eq}}$.

We consider a linearly-polarized light, and define x axis parallel to the polarization direction. Then the electric field can be described by $\mathbf{A}(t) = A(t)\hat{x}$ (\hat{x} : a unit vector along x axis) which gives

$$\delta b_{\gamma\mathbf{k}}^z(\omega) = \frac{e^2}{2}A^2(\omega)\frac{\partial^2\epsilon_{\gamma\mathbf{k}}}{\partial k_x^2}, \quad (19)$$

where $A^2(\omega)$ is the Fourier transform of $A(t)^2$. The above pseudospin formulation can be regarded as a linear-response theory to a “nonlinear” field $A(t)^2$. In the following sections, we shall solve the linearized Eq.(18) self-consistently.

III. OPTICAL EXCITATION OF LEGGETT MODES

First we derive the solution for the imaginary parts of the gaps. Summing $\delta\sigma_{\gamma\mathbf{k}}^x(\omega)$ along Eq.(18) and using the self-consistent constraint Eq.(10), we obtain

$$\begin{pmatrix} \delta\Delta''_{\alpha}(\omega) \\ \delta\Delta''_{\beta}(\omega) \end{pmatrix} = \frac{e^2 A^2(\omega)}{i\omega [\omega^2 F_{\alpha}(\omega) F_{\beta}(\omega) \det \lambda + \lambda_{\beta\alpha} \Delta_{\alpha} F_{\alpha}(\omega) + \lambda_{\alpha\beta} \Delta_{\beta} F_{\beta}(\omega)]} \\ \times \begin{pmatrix} \omega^2 F_{\beta}(\omega) \det \lambda + \lambda_{\beta\alpha} \Delta_{\alpha} & \lambda_{\alpha\beta} \Delta_{\alpha} \\ \lambda_{\beta\alpha} \Delta_{\beta} & \omega^2 F_{\alpha}(\omega) \det \lambda + \lambda_{\alpha\beta} \Delta_{\beta} \end{pmatrix} \begin{pmatrix} \Delta_{\alpha} Y_{\alpha}(\omega) \\ \Delta_{\beta} Y_{\beta}(\omega) \end{pmatrix}, \quad (20)$$

where

$$F_{\gamma}(\omega) = \frac{1}{D_{\gamma}} \sum_{\mathbf{k}} \frac{\sigma_{\gamma\mathbf{k}}^x}{4E_{\gamma\mathbf{k}}^2 - \omega^2}, \quad (21)$$

$$Y_{\gamma}(\omega) = \frac{1}{D_{\gamma}} \sum_{\mathbf{k}} \frac{\sigma_{\gamma\mathbf{k}}^x}{4E_{\gamma\mathbf{k}}^2 - \omega^2} \frac{\partial^2 \epsilon_{\gamma\mathbf{k}}}{\partial k_x^2}, \quad (22)$$

$$\lambda_{\gamma\gamma'} = V_{\gamma\gamma'} D_{\gamma'}, \quad \det \lambda = \lambda_{\alpha\alpha} \lambda_{\beta\beta} - \lambda_{\alpha\beta} \lambda_{\beta\alpha}, \quad (23)$$

with

$$D_{\gamma} = \sum_{\mathbf{k}} \delta(\epsilon - \epsilon_{\gamma\mathbf{k}}) \quad (24)$$

being the density of states on the Fermi surface of γ -band, assumed to be constant around the Fermi energy ($\epsilon \approx 0$). We will summarize the definition of symbols such as Eqs.(21)-(24) in Appendix.

We replace the \mathbf{k} summation with an energy integral,

$$\sum_{\mathbf{k}} = \int d\epsilon \sum_{\mathbf{k}} \delta(\epsilon - \epsilon_{\gamma\mathbf{k}}), \quad (25)$$

to obtain

$$F_{\gamma}(\omega) = \int_{-\infty}^{\infty} d\epsilon \frac{\Delta_{\gamma} \tanh\left(\sqrt{\epsilon^2 + \Delta_{\gamma}^2}/2k_B T\right)}{2\sqrt{\epsilon^2 + \Delta_{\gamma}^2} (4\epsilon^2 + 4\Delta_{\gamma}^2 - \omega^2)}, \quad (26)$$

$$Y_{\gamma}(\omega) = c_{\gamma 0} F_{\gamma}(\omega), \quad (27)$$

where the coefficient $c_{\gamma 0}$ is defined by a series expansion

$$\sum_{\mathbf{k}} \delta(\epsilon - \epsilon_{\gamma\mathbf{k}}) \frac{\partial^2 \epsilon_{\gamma\mathbf{k}}}{\partial k_x^2} = D_{\gamma} (c_{\gamma 0} + c_{\gamma 1} \epsilon + c_{\gamma 2} \epsilon^2 \dots). \quad (28)$$

We have neglected higher-order coefficients $c_{\gamma n}$ with $n \geq 2$ to derive Eq.(27), which is valid as long as the vicinity of the Fermi surface is concerned.

The formalism presented here is general enough to be applicable to any band structures. It also describes the polarization dependence of the optical response, since the coefficients $\{c_{\gamma n}\}$ change according to the relative angles between x axis (polarization direction of the incident light) and the crystallographic axes.

In the linearized Eqs.(15)-(17), the imaginary part of Δ_{γ} is proportional to the phase θ_{γ} defined by $\Delta_{\gamma} = |\Delta_{\gamma}| e^{i\theta_{\gamma}}$. The phase difference between the two gaps is a physical (gauge-invariant) quantity, while each phase is not. Motion of the phase difference is governed by

$$\delta[\theta_{\alpha}(\omega) - \theta_{\beta}(\omega)] = \frac{\delta\Delta''_{\alpha}(\omega)}{\Delta_{\alpha}} - \frac{\delta\Delta''_{\beta}(\omega)}{\Delta_{\beta}} = -e^2 A^2(\omega) i\omega L(\omega), \quad (29)$$

where

$$L(\omega) = \frac{(c_{\alpha 0} - c_{\beta 0}) F_{\alpha}(\omega) F_{\beta}(\omega) \det \lambda}{\omega^2 F_{\alpha}(\omega) F_{\beta}(\omega) \det \lambda + \lambda_{\beta\alpha} \Delta_{\alpha} F_{\alpha}(\omega) + \lambda_{\alpha\beta} \Delta_{\beta} F_{\beta}(\omega)}. \quad (30)$$

This solution describes *resonance between the squared electric field and the Leggett mode*, whose energy is determined by the frequency at which the denominator of Eq.(30) vanishes³⁴,

$$\omega^2 F_{\alpha}(\omega) F_{\beta}(\omega) \det \lambda + \lambda_{\beta\alpha} \Delta_{\alpha} F_{\alpha}(\omega) + \lambda_{\alpha\beta} \Delta_{\beta} F_{\beta}(\omega) = 0. \quad (31)$$

For weak enough $V_{\alpha\beta}$, Eq.(31) has a solution,

$$\omega^2 = \omega_L^2 \equiv -4 \left(\frac{\lambda_{\alpha\beta} + \lambda_{\beta\alpha}}{\det \lambda} \right) \Delta_{\alpha} \Delta_{\beta}, \quad (32)$$

at $T = 0$, where $F_{\gamma}(\omega)$ reduces to

$$F_{\gamma}(\omega) = \frac{\Delta_{\gamma}}{\omega \sqrt{4\Delta_{\gamma}^2 - \omega^2}} \sin^{-1} \left(\frac{\omega}{2|\Delta_{\gamma}|} \right). \quad (33)$$

The right-hand side of Eq.(32) is positive-definite, because $V_{\alpha\beta}/\det V$ and $\Delta_{\alpha}\Delta_{\beta}$ necessarily have opposite signs (see the previous section). The mode energy (32) was originally derived by Leggett²². We consider a monochromatic wave turned on at $t = 0$, $A(t > 0) = A_0 \sin \Omega t$, for which the Fourier transform of the squared vector potential is given by

$$A^2(\omega) = \frac{4A_0^2 \Omega^2}{i\omega (4\Omega^2 - \omega^2)}, \quad (34)$$

where ω on the right-hand side stands for $\omega - i0$. Then, in the limit of small $V_{\alpha\beta}$, we can show that approximately

$$\delta[\theta_{\alpha} - \theta_{\beta}] \simeq \frac{4(c_{\alpha 0} - c_{\beta 0}) \Omega^2 e^2 A_0^2}{(\omega^2 - 4\Omega^2)(\omega^2 - \omega_L^2)}. \quad (35)$$

An inverse Fourier transform gives the temporal behavior,

$$\delta[\theta_{\alpha} - \theta_{\beta}] \simeq \frac{4(c_{\alpha 0} - c_{\beta 0}) \Omega^2 e^2 A_0^2}{4\Omega^2 - \omega_L^2} \left(\frac{\sin \omega_L t}{\omega_L} - \frac{\sin 2\Omega t}{2\Omega} \right), \quad (36)$$

for $t > 0$. When 2Ω (the incident wave frequency doubled) is close to ω_L , the poles ($\omega = \pm 2\Omega, \pm \omega_L$) on the right-hand side of Eq.(35) merge, leading to a resonance

between the Leggett mode and forced oscillation due to the electromagnetic wave. In the time domain, it appears as a factor $(4\Omega^2 - \omega_L^2)$ in the denominator of Eq.(36), which enhances both the forced oscillation and the excited Leggett mode. Under the exact resonance condition, $2\Omega = \omega_L$, Eq.(35) gives

$$\delta[\theta_\alpha - \theta_\beta] \simeq \frac{(c_{\alpha 0} - c_{\beta 0})\omega_L^2 e^2 A_0^2}{2} \left(\frac{\sin \omega_L t}{\omega_L} - t \cos \omega_L t \right), \quad (37)$$

whose amplitude diverges for $t \rightarrow \infty$ (so that, strictly speaking, the linearized equation of motion fails in the exact resonance and nonlinear effects will dominate in the long-time behavior). This provides a new concept of *resonant excitation of Leggett mode*.

In the limit of small $V_{\alpha\beta}$, the Leggett mode has an infinite lifetime since the first term in the right-hand side of Eq.(36) does not decay. However, stronger interband coupling increases the energy of Leggett mode, and when it exceeds the smaller of $2|\Delta_\alpha|$ and $2|\Delta_\beta|$, the mode becomes short-lived. To see this, we examine the spectral feature of $L(\omega)$, which can be regarded as the resonance factor for the Leggett mode. As a measure of the interband coupling strength, we define a dimensionless quantity,

$$\lambda_I \equiv V_{\alpha\beta} \sqrt{D_\alpha D_\beta}, \quad (38)$$

with $\lambda_I^2 = \lambda_{\alpha\beta} \lambda_{\beta\alpha}$. When the sign of λ_I (i.e., the sign of $V_{\alpha\beta}$) is inverted, the sign of $\Delta_\alpha \Delta_\beta$ is also changed (since $V_{\alpha\beta}/\det V$ and $\Delta_\alpha \Delta_\beta$ have opposite signs in the ground state as mentioned), but this is cancelled between the denominator and numerator in Eq.(30) so that $L(\omega)$ remains the same for positive and negative λ_I . Figure 1 illustrates the absolute value of $L(\omega)$ at $T = 0$ for $0 \leq |\lambda_I| \leq 0.071$ (Fig. 1(a)), and $0.095 \leq |\lambda_I| \leq 0.38$ (Fig. 1(b)) with $c_{\alpha 0} - c_{\beta 0} = 1$. The parameters are taken to be $\lambda_{\alpha\alpha} = -0.28$, $\lambda_{\beta\beta} = -0.96$, $\lambda_{\alpha\beta}/\lambda_{\beta\alpha} = D_\beta/D_\alpha = 0.73$, $\Delta_\alpha/\omega_c = 0.31$, $\Delta_\beta/\omega_c = 0.96$, which are chosen for MgB_2 ^{29,31,34}, where the interband interaction $\lambda_I = -0.19$ is estimated from Ref.31. Energy is measured in units of the cut-off energy ω_c , which is necessary to obtain a finite solution of the BCS gap equation. Here we intended to look into the peak positions relative to the gap function, so that we show the result when the modification of Δ_γ by changing λ_I through the gap equation is ignored. We have qualitatively similar behavior for $|L(\omega)|$ (peak widths, etc.) when we take account of that.

When the interband coupling is relatively small, Eq.(31) has a real solution smaller than $2\Delta_\alpha$ so that $|L(\omega)|$ diverges as shown in Fig. 1(a). This contrasts with the case of the relatively strong interband coupling, where Eq.(31) has no real solution and thus $|L(\omega)|$ does not diverge as shown in Fig. 1(b). Instead, $|L(\omega)|$ is peaked at a frequency above $2\Delta_\alpha$. We define the peak frequency ω_L as the energy of the Leggett mode, and plot ω_L and the halfwidth of $|L(\omega)|$ against $|\lambda_I|$ in Fig. 2. For small $|\lambda_I|$, $|L(\omega)|$ diverges at $\omega = \omega_L$ as determined by

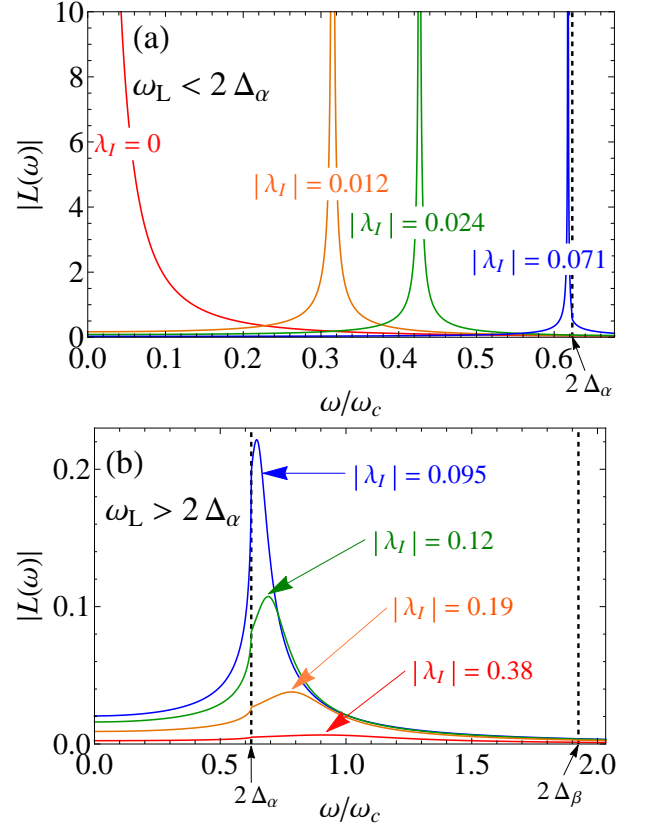


FIG. 1. $|L(\omega)|$ at $T = 0$ for several values of the dimensionless interband pairing interaction $|\lambda_I|$ varied from 0 to 0.071 (a) and from 0.095 to 0.38 (b), for $\lambda_{\alpha\alpha} = -0.28$, $\lambda_{\beta\beta} = -0.96$, $\lambda_{\alpha\beta}/\lambda_{\beta\alpha} = 0.73$, $\Delta_\alpha/\omega_c = 0.31$, $\Delta_\beta/\omega_c = 0.96$, and $c_{\alpha 0} - c_{\beta 0} = 1$. Position of the peak defines ω_L .

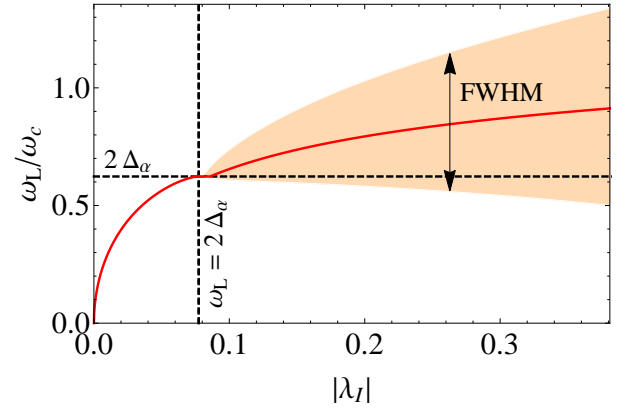


FIG. 2. The energy of the Leggett mode (red line) and halfwidth (full width at half maximum; FWHM) of $|L(\omega)|$ (orange regions) against the interband pairing interaction $|\lambda_I|$. The horizontal dashed line indicates the smaller gap $2\Delta_\alpha$, while the vertical one the critical value of $|\lambda_I|$ at which ω_L reaches $2\Delta_\alpha$. Values of the used parameters are the same as in Fig. 1.

the solution of Eq.(31), so that the halfwidth is ill-defined (or zero). By contrast, when ω_L exceeds the smaller gap $2\Delta_\alpha$ as λ_I is increased, $|L(\omega)|$ stops diverging and starts to have finite widths, where both ω_L and the halfwidth increase monotonically with $|\lambda_I|$. Since the lifetime of the mode is roughly given by the inverse of the halfwidth, one can say that the Leggett mode is a long-lived mode only when its energy is below the superconducting gaps. This is due to suppression of the decay from the Leggett mode to lower-energy quasi-particles³⁵.

Even when the lifetime of the Leggett mode is finite, the peak of $|L(\omega)|$ at $\omega = \omega_L$ and the pole of $A^2(\omega)$ at $\omega = 2\Omega$ can constructively enhance the optical response in Eq.(29). Thus a resonant excitation of the Leggett mode is also available for short-lived cases, while sharpness of the resonance will be degraded.

The mechanism of the *light-induced Leggett mode* found here can be explained as follows. In the absence of $V_{\alpha\beta}$, Eq.(20) drives a rotation of the phases in the form of

$$\Delta_\gamma(t) = \Delta_\gamma(0) \exp\left(ic_{\gamma 0} e^2 \int_0^t dt' A(t')^2\right). \quad (39)$$

This implies that a Cooper pair with charge $2e$ in γ -band feels an effective electrostatic potential $\Phi_\gamma^{\text{eff}} =$

$(c_{\gamma 0}/2)eA(t)^2$. In single-band superconductors, this phase can be gauged out¹⁹, and the effective potential has no physical meaning. By contrast, a two-band system has two phase variables, which cannot be simultaneously gauged out, with the phase difference being invariant under the gauge transformation. Correspondingly, a difference in the effective potential between the two bands has a physical effect: when $c_{\alpha 0} \neq c_{\beta 0}$, an effective voltage emerges between the two bands, leading to a phase difference between the gaps. In the presence of $\lambda_I \neq 0$, however, a particular relation (s_\pm or s_{++}) is imposed upon the ground state as discussed around Eq.(11), so that any phase difference produces a restoring force. This restoring force acts to induce the Leggett mode.

IV. OPTICAL EXCITATION OF HIGGS MODES

Now we move on to the real parts of the gaps. The self-consistent solution of Eq.(18) is given by

$$\begin{pmatrix} \delta\Delta'_\alpha(\omega) \\ \delta\Delta'_\beta(\omega) \end{pmatrix} = \frac{e^2 A^2(\omega)}{2} \begin{pmatrix} H_\alpha(\omega) \\ H_\beta(\omega) \end{pmatrix}, \quad (40)$$

where we have defined

$$\begin{pmatrix} H_\alpha(\omega) \\ H_\beta(\omega) \end{pmatrix} = - \frac{1}{G_\alpha(\omega)G_\beta(\omega) \det \lambda - \lambda_{\beta\alpha}\Delta_\alpha G_\alpha(\omega) - \lambda_{\alpha\beta}\Delta_\beta G_\beta(\omega)} \\ \times \begin{pmatrix} G_\beta(\omega) \det \lambda - \lambda_{\beta\alpha}\Delta_\alpha & -\lambda_{\alpha\beta}\Delta_\alpha \\ -\lambda_{\beta\alpha}\Delta_\beta & G_\alpha(\omega) \det \lambda - \lambda_{\alpha\beta}\Delta_\beta \end{pmatrix} \begin{pmatrix} \Delta_\alpha X_\alpha(\omega) \\ \Delta_\beta X_\beta(\omega) \end{pmatrix}, \quad (41)$$

$$G_\gamma(\omega) = (4\Delta_\gamma^2 - \omega^2)F_\gamma(\omega), \quad (42)$$

$$X_\gamma(\omega) = \frac{1}{D_\gamma} \sum_{\mathbf{k}} \frac{4\sigma_{\gamma\mathbf{k}}^x \epsilon_{\gamma\mathbf{k}}}{4E_{\gamma\mathbf{k}}^2 - \omega^2} \frac{\partial^2 \epsilon_{\gamma\mathbf{k}}}{\partial k_x^2} \\ = -c_{\gamma 1} \left[\frac{\lambda_{\gamma\bar{\gamma}}\Delta_\gamma - \lambda_{\gamma\bar{\gamma}}\Delta_{\bar{\gamma}}}{\det \lambda} + G_\gamma(\omega) \right], \quad (43)$$

with $c_{\gamma 1}$ defined by Eq.(28), and $\bar{\alpha} = \beta$, $\bar{\beta} = \alpha$. The function $H_\gamma(\omega)$ ($\gamma = \alpha, \beta$) describes resonance between the squared electric field and the Higgs modes, while $X_\gamma(\omega)$ gives rise to coupling between them.

We plot $|H_\gamma(\omega)|$ in Fig. 3, for $c_{\alpha 1} = c_{\beta 1} = -1$ and the parameters estimated for MgB₂ as in Fig. 1. Here, too, we have shown the result when the modification of Δ_γ by changing λ_I is ignored, while qualitatively similar behavior is obtained when we take account of that. The peaks at $\omega = 2\Delta_\alpha$, $2\Delta_\beta$ (which we call $\omega_{H\alpha}$ and $\omega_{H\beta}$, respectively) represent the Higgs modes. Due to interband interaction, they are coupled to each other, so that both of $|H_\gamma(\omega)|$ show the two peaks for finite λ_I (while they approach the two separated single-band Higgs modes¹⁹ in the limit $\lambda_I \rightarrow 0$). As in the single-

band case^{18,19} and the Leggett mode discussed in the previous section, the Higgs modes in two-band superconductors can be resonantly excited by electromagnetic waves at $2\Omega \simeq \omega_{H\alpha}$, $\omega_{H\beta}$. The two Higgs modes, however, show very different resonance features. $|H_\beta(\omega)|$ has a sharp resonance peak at $\omega = 2\Delta_\beta$ for all values of λ_I chosen, though the peak height somewhat decreases. By contrast, the peak of $|H_\alpha(\omega)|$ at $\omega = 2\Delta_\alpha$ is more rapidly lowered and broadened with increasing $|\lambda_I|$, and finally disappears [Fig.3(a), blue curve]. We summarize the peak positions and halfwidths of $|H_\gamma(\omega)|$ in Fig. 4. Unlike the relatively narrow width of $|H_\beta(\omega)|$ around $\omega = 2\Delta_\beta$, the peak of $|H_\alpha(\omega)|$ at $\omega = 2\Delta_\alpha$ becomes rapidly broadened as $|\lambda_I|$ is increased, and when $|\lambda_I|$ exceeds a certain value, the “width” can no longer be defined. If we further increase $|\lambda_I|$, the peak vanishes at a certain point. This indicates that the Higgs mode associated with the larger gap is relatively more stable than the one associated with the lower gap, contrary to a naive expectation that a lower-energy excitation would be more stable.

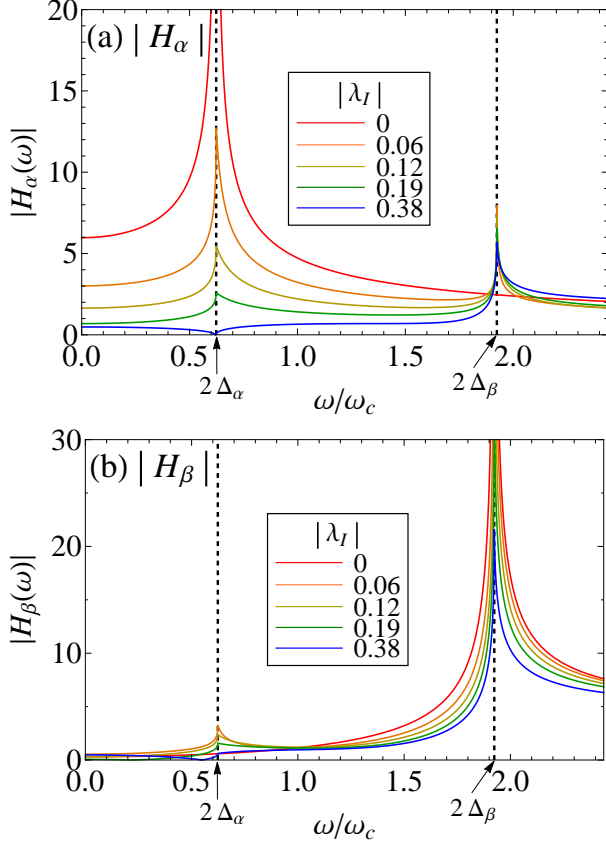


FIG. 3. $|H_\alpha(\omega)|$ (a) and $|H_\beta(\omega)|$ (b) for several values of $|\lambda_I|$ varied from 0 to 0.38, with $c_{\alpha 1} = c_{\beta 1} = -1$ and the same parameters as Fig. 1.

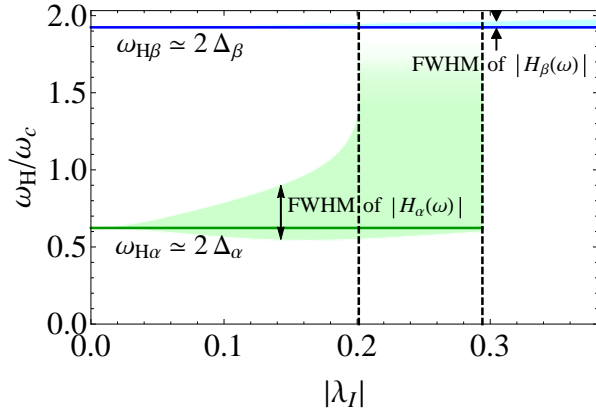


FIG. 4. Dependence of the Higgs modes on the interband pairing interaction $|\lambda_I|$. Green (blue) line represents the mode energy $\omega_{H\alpha}$ ($\omega_{H\beta}$), defined as the peak of $|H_\alpha(\omega)|$ ($|H_\beta(\omega)|$), associated with the smaller gap $2\Delta_\alpha$ (larger gap $2\Delta_\beta$). The halfwidths are indicated by green (blue) regions. Left dashed line indicates $|\lambda_I|$ at which the upper halfwidth of $|H_\alpha(\omega)|$ diverges, while the right one the $|\lambda_I|$ at which the peak of $|H_\alpha(\omega)|$ at $\omega = 2\Delta_\alpha$ disappears. Used parameters are the same as Fig. 3.

The reason why the Higgs mode with the lower energy disappears can be explained as follows. For small $|\lambda_I|$, the two condensates, hence the two Higgs modes, are almost independent of each other. For strong enough $|\lambda_I|$, on the other hand, the two condensates are so strongly coupled that they can be regarded as almost one condensate. Its character is dominated by the component having the larger superfluid density, hence the larger gap. Therefore, only one Higgs mode with the higher energy survives for large enough interband interactions.

V. TEMPERATURE EFFECTS ON MODE RESONANCES

The effect of temperature on the sharpness of resonances is an important issue, especially from experimental points of view. It is also directly associated with the stability of the Leggett and Higgs modes, because the resonance widths are associated with lifetimes of excitations. To explore this, here we have numerically solved the gap Eqs.(10, 12) incorporating the effect of interband coupling λ_I to calculate Eq.(26), for the values of parameters estimated for MgB_2 , $\lambda_I = -0.19$, etc [see section III]. We can then obtain $L(\omega)$ and $H_\gamma(\omega)$ that are valid at finite temperatures. In Fig. 5, panel (a) depicts the temperature dependence of the gap energies against temperature. We then plot $|L(\omega)|$ and $|H_\gamma(\omega)|$ at several temperatures as indicated by horizontal lines in panel (a). In panel (b) we can see that the peak of $|L(\omega)|$ becomes sharper as temperature increases, which indicates a stabilization of the Leggett mode. This contrasts with the peak of $|H_\alpha(\omega)|$ at $\omega = 2\Delta_\alpha$ in panel (c), which is weakened and finally disappears with increasing temperature. The peak of $|H_\beta(\omega)|$ at $\omega = 2\Delta_\beta$ in (d) remains sharp even at finite temperatures.

We summarize these by plotting the peak positions and widths for $|L(\omega)|$ and $|H_\gamma(\omega)|$ against temperature in Fig. 6. At $T = 0$, the Leggett mode has an energy ω_L between the two superconducting gaps $2\Delta_\alpha$ and $2\Delta_\beta$, and has a broad width as already mentioned. As ω_L decreases with increasing temperature, the mode energy reaches the lower gap $2\Delta_\alpha$ at a certain point. At even higher temperatures, the mode energy ω_L traces $2\Delta_\alpha$ with a slightly narrowing width. As for the Higgs modes, their energies follow the temperature dependence of the gaps, which can be understood in terms of Eq.(41) with $G_\gamma(\omega = 2\Delta_\gamma) = 0$. The Higgs mode with higher energy has quite narrow widths for the whole temperature range, which reveals that the Higgs mode with the higher energy remains long-lived. On the other hand, the width of the Higgs mode with lower energy is broadened as temperature is increased, and the peak of this mode disappears at a certain temperature.

Sharpening of the Leggett mode might seem to arise because the mode becomes one of the lowest-energy excitations and thus a stable mode at high temperatures. However, this cannot explain the broadening and disap-

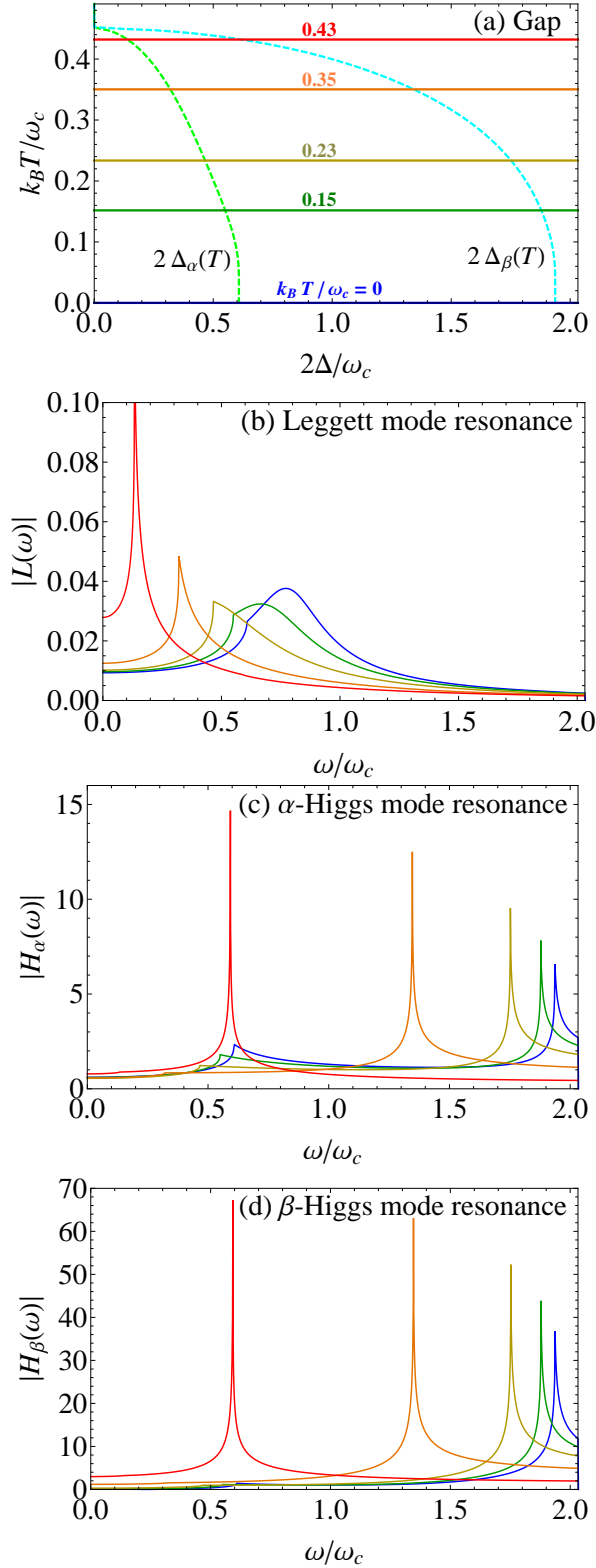


FIG. 5. Dependence of the gaps (horizontal axis) $2\Delta_\alpha(T)$ and $2\Delta_\beta(T)$ (green and blue dotted lines, respectively) against temperature (vertical axis), for $\lambda_{\alpha\alpha} = -0.28$, $\lambda_{\beta\beta} = -0.96$, $\lambda_{\alpha\beta}/\lambda_{\beta\alpha} = 0.73$ and $\lambda_I = -0.19$ (a). Temperatures chosen in panels (b-d) are indicated by horizontal lines: $k_B T/\omega_c = 0$ (blue), 0.15 (green), 0.23 (khaki), 0.35 (orange), and 0.43 (red). $|L(\omega)|$ (b), $|H_\alpha(\omega)|$ (c) and $|H_\beta(\omega)|$ (d) for several values of T with $c_{\alpha 0} - c_{\beta 0} = 1$ and $c_{\alpha 1} = c_{\beta 1} = -1$.

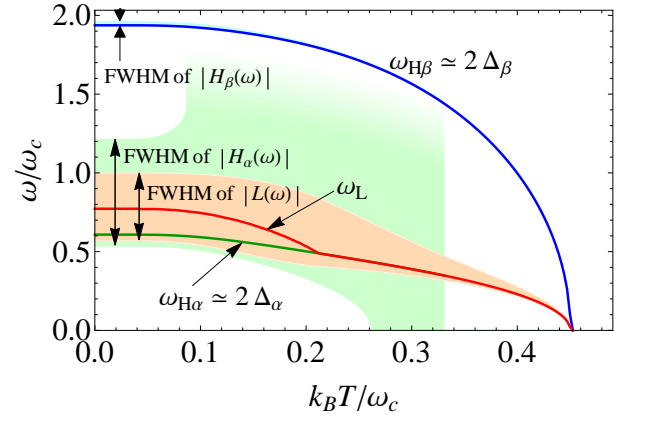


FIG. 6. Temperature dependence of the Leggett mode energy ω_L (red line) and the Higgs mode energies $\omega_{H\alpha}$ (green), and $\omega_{H\beta}$ (blue). Their resonance widths are indicated by orange, green and blue regions, respectively. The green line denoting $\omega_{H\alpha}$ overlaps with the red line up to the right edge of the green region, at which the green line is terminated. Used parameters are the same as Fig. 5.

pearance of the lower-energy Higgs mode, which is also degenerate with the lowest-energy excitations. Rather, this can be intuitively explained as follows. At low temperatures, Cooper pairs are basically formed through the intraband interactions, giving rise to Higgs modes primarily associated with each band (although modifications due to the interband coupling, such as a broadening of the lower-energy Higgs mode, exist). At higher temperatures, however, Cooper pairs with the smaller gap could no longer be formed if it were not for the interband coupling, since the ordinary single-band BCS theory predicts a lower critical temperature for a smaller superconducting gap. Through a nonzero interband coupling, the larger gap $2\Delta_\beta$ makes the lower $2\Delta_\alpha$ finite even at higher temperatures, but Cooper pairs are robbed of α -band character there, and only the Higgs mode associated with the larger gap remains.

VI. THIRD-HARMONIC GENERATION FROM LIGHT-INDUCED COLLECTIVE MODES

Matsunaga *et al.*¹⁸ have experimentally revealed that a conventional superconductor NbN illuminated with an intense THz wave emits the third-harmonic. This is an intrinsic nonlinear phenomenon in superconductors^{19,45}. As mentioned in Sec. II, Anderson's pseudospins describing Cooper pairs respond to $A(t)^2$. Such pseudospin motions induce an electric current which is itself proportional to $A(t)$ (as shown later). The induced current thus follows $\sim A(t)^3$ in total, and emits the third-harmonic, which can be and has been detected by a simple transmission experiment. In single-band superconductors, THG is resonantly enhanced when the doubled frequency of

the pump light coincides with the superconducting gap 2Δ ; the THG resonance occurs due to both the Higgs mode and density fluctuations, the latter being shown to be dominant within the BCS theory⁴⁵. We can raise an intriguing question of how THG should look like in two-band superconductors.

Amplitude of the emitted electric field is proportional to the induced current, so let us calculate the light-induced third-order current. The total electric current is expressed as

$$\begin{aligned} \mathbf{j} &= e \sum_{\gamma \mathbf{k} \sigma} [\nabla_{\mathbf{k}} \epsilon_{\gamma(\mathbf{k}-e\mathbf{A})}] \gamma_{\mathbf{k}\sigma}^\dagger \gamma_{\mathbf{k}\sigma} \\ &= e \sum_{\gamma \mathbf{k}} [\nabla_{\mathbf{k}} \epsilon_{\gamma(\mathbf{k}-e\mathbf{A})} - \nabla_{\mathbf{k}} \epsilon_{\gamma(\mathbf{k}+e\mathbf{A})}] \left(\sigma_{\gamma \mathbf{k}}^z + \frac{1}{2} \right) \\ &\quad + e \sum_{\gamma \mathbf{k}} [\nabla_{\mathbf{k}} \epsilon_{\gamma(\mathbf{k}-e\mathbf{A})} + \nabla_{\mathbf{k}} \epsilon_{\gamma(\mathbf{k}+e\mathbf{A})}] \left(\sigma_{\gamma \mathbf{k}}^x - \frac{1}{2} \right), \end{aligned} \quad (44)$$

where

$$\sigma_{\gamma \mathbf{k}}^x = \frac{1}{2} (\gamma_{\mathbf{k}\uparrow}^\dagger \gamma_{-\mathbf{k}\downarrow}) \mathbf{1} \begin{pmatrix} \gamma_{\mathbf{k}\uparrow} \\ \gamma_{-\mathbf{k}\downarrow}^\dagger \end{pmatrix} \quad (45)$$

remains constant during time evolution in the mean-field Hamiltonian (4). Because $\sigma_{\gamma \mathbf{k}}(t)$ responds to $A(t)^2$, forced oscillations of $\delta\sigma_{\gamma \mathbf{k}}^z(t)$ have a frequency 2Ω for the incident frequency Ω of $A(t)$. The first term in Eq.(44) thus accommodates a third-harmonic component with a frequency 3Ω ,

$$j^{(3)i}(t) = -2e^2 A(t) \sum_{\gamma} \sum_{\mathbf{k}} \frac{\partial^2 \epsilon_{\gamma \mathbf{k}}}{\partial k_i \partial k_x} \delta\sigma_{\gamma \mathbf{k}}^z(t), \quad (46)$$

where $i = x, y, \dots$ denotes spatial directions. According to Eq.(18),

$$\begin{aligned} j^{(3)i}(t) &= -2e^2 A(t) \int \frac{d\omega}{2\pi} e^{i\omega t} \sum_{\gamma} \sum_{\mathbf{k}} \frac{\partial^2 \epsilon_{\gamma \mathbf{k}}}{\partial k_i \partial k_x} \frac{\sigma_{\gamma \mathbf{k}}^x}{4E_{\gamma \mathbf{k}}^2 - \omega^2} \\ &\quad \times [4\epsilon_{\gamma \mathbf{k}} \delta\Delta'_{\gamma}(\omega) + 2i\omega \delta\Delta''_{\gamma}(\omega) - 4\Delta_{\gamma} \delta b_{\gamma \mathbf{k}}^z(\omega)]. \end{aligned} \quad (47)$$

The first term in the bracket on the right-hand side corresponds to the Higgs mode contribution¹⁹, while the last term the contribution from density fluctuations⁴⁵. The second term gives a phase contribution, which is screened in the case of single-band superconductors. We denote the Higgs mode, phase and density fluctuation contributions as $\mathbf{j}_H^{(3)}$, $\mathbf{j}_L^{(3)}$ and $\mathbf{j}_d^{(3)}$, respectively, where the subscript ‘‘L’’ denotes the Leggett mode because the phase contribution is related to this mode as discussed later. Then the total third-order current reads

$$\mathbf{j}^{(3)}(t) = \mathbf{j}_H^{(3)}(t) + \mathbf{j}_L^{(3)}(t) + \mathbf{j}_d^{(3)}(t). \quad (48)$$

With the use of Eq.(40) and a function (43), the Higgs

mode contribution is reduced to

$$\begin{aligned} j_H^{(3)i}(t) &= -e^4 A(t) \sum_{\gamma} \frac{c_{\gamma 1}^i}{c_{\gamma 1}} D_{\gamma} \\ &\quad \times \int \frac{d\omega}{2\pi} e^{i\omega t} A^2(\omega) H_{\gamma}(\omega) X_{\gamma}(\omega), \end{aligned} \quad (49)$$

where $c_{\gamma 1}^i$ is defined by

$$\sum_{\mathbf{k}} \delta(\epsilon - \epsilon_{\gamma \mathbf{k}}) \frac{\partial^2 \epsilon_{\gamma \mathbf{k}}}{\partial k_i \partial k_x} = D_{\gamma} (c_{\gamma 0}^i + c_{\gamma 1}^i \epsilon + \dots). \quad (50)$$

As before, x is the polarization direction of the incident light. For $i = x$, Eq.(50) is equivalent to Eq.(28), hence $c_{\gamma n}^x = c_{\gamma n}$ ($n = 0, 1, \dots$). While $X_{\gamma}(\omega)$ has no distinctive spectral features, $H_{\gamma}(\omega)$ has peak structures around $\omega = 2|\Delta_{\alpha, \beta}|$ which represent the two Higgs modes, so that the third-harmonic arising from Eq.(49) is resonantly enhanced at $2\Omega \approx 2|\Delta_{\alpha, \beta}|$. For strong interband interactions for which the Higgs mode with the lower energy is overdamped, the corresponding THG will be negligible as compared with the higher-energy one.

Now we turn to the other contributions. Using Eqs.(19, 20, 27, 30), the phase and density-fluctuation contributions are reduced, respectively, to

$$\begin{aligned} j_L^{(3)i}(t) &= 4e^4 A(t) \\ &\quad \times \left[(c_{\alpha 0}^i - c_{\beta 0}^i) \frac{\lambda_I \sqrt{D_{\alpha} D_{\beta}} \Delta_{\alpha} \Delta_{\beta}}{\det \lambda} \int \frac{d\omega}{2\pi} e^{i\omega t} A^2(\omega) L(\omega) \right. \\ &\quad \left. - \sum_{\gamma} c_{\gamma 0}^i c_{\gamma 0} D_{\gamma} \Delta_{\gamma} \int \frac{d\omega}{2\pi} e^{i\omega t} A^2(\omega) F_{\gamma}(\omega) \right], \end{aligned} \quad (51)$$

$$j_d^{(3)i}(t) = 4e^4 A(t) \sum_{\gamma} \tilde{c}_{\gamma 0} D_{\gamma} \Delta_{\gamma} \int \frac{d\omega}{2\pi} e^{i\omega t} A^2(\omega) F_{\gamma}(\omega), \quad (52)$$

with $c_{\gamma 0}^i$ defined by Eq.(50) and $\tilde{c}_{\gamma 0}^i$ by

$$\sum_{\mathbf{k}} \delta(\epsilon - \epsilon_{\gamma \mathbf{k}}) \frac{\partial^2 \epsilon_{\gamma \mathbf{k}}}{\partial k_i \partial k_x} \frac{\partial^2 \epsilon_{\gamma \mathbf{k}}}{\partial k_x^2} = D_{\gamma} (\tilde{c}_{\gamma 0}^i + \tilde{c}_{\gamma 1}^i \epsilon + \dots). \quad (53)$$

We can show that, when we take account of the screening due to the long-range Coulomb interaction, the term represented by the third line in Eq.(51) is screened out, while the same term appears as a screening effect in Eq.(52)⁴⁷. Thus we have a screened form as

$$\begin{aligned} j_L^{(3)i}(t) &= 4e^4 A(t) (c_{\alpha 0}^i - c_{\beta 0}^i) \frac{\lambda_I \sqrt{D_{\alpha} D_{\beta}} \Delta_{\alpha} \Delta_{\beta}}{\det \lambda} \\ &\quad \times \int \frac{d\omega}{2\pi} e^{i\omega t} A^2(\omega) L(\omega), \end{aligned} \quad (54)$$

$$\begin{aligned} j_d^{(3)i}(t) &= 4e^4 A(t) \sum_{\gamma} (\tilde{c}_{\gamma 0}^i - c_{\gamma 0}^i c_{\gamma 0}) D_{\gamma} \Delta_{\gamma} \\ &\quad \times \int \frac{d\omega}{2\pi} e^{i\omega t} A^2(\omega) F_{\gamma}(\omega). \end{aligned} \quad (55)$$

Equation (54) can be reduced to

$$j_L^{(3)i}(t) = -4e^2 A(t) (c_{\alpha 0}^i - c_{\beta 0}^i) \frac{\lambda_I \sqrt{D_\alpha D_\beta} \Delta_\alpha \Delta_\beta}{\det \lambda} \times \int_{-\infty}^t dt' \delta[\theta_\alpha(t') - \theta_\beta(t')] \quad (56)$$

with the use of Eq.(29). As already shown, forced oscillation of the phase difference $\delta[\theta_\alpha(t) - \theta_\beta(t)]$ resonates with the Leggett mode at $2\Omega \approx \omega_L$, so that Eq.(56) and the resulting third-harmonic is enhanced on the same condition. Thus this current represents *THG from resonantly excited Leggett mode*. Presence of this phase contribution sharply contrasts with the single-band cases where the phase contribution is fully screened out.

On the other hand, Eq.(55) for $j_d^{(3)}$ is resonantly enhanced at $2\Omega \approx 2|\Delta_{\alpha,\beta}|$, because $F_\gamma(\omega)$ diverges at $\omega = 2|\Delta_\gamma|$ following $F_\gamma(\omega) \sim 1/\sqrt{4\Delta_\gamma^2 - \omega^2}$ [which can be seen in Eq.(33)]. Intuitively, this is due to a resonance between $A(t)^2$ and Bogoliubov quasi-particles at the superconducting gap edge with diverging density of states. We have called its origin “density fluctuations,” because it has a form of density-density correlation function. In view of Eq.(55), $F_\gamma(\omega)$ can be regarded as the resonance factor for density fluctuations.

All of the Higgs, Leggett modes and density fluctuations thus contribute to THG. Both of the Higgs modes and density fluctuations exhibit THG resonance at $2\Omega \simeq 2\Delta_{\alpha,\beta}$, which makes it difficult to experimentally distinguish them simply from the resonance frequency (while the Leggett mode resonance at $2\Omega \simeq \omega_L$ may be distinguishable). However, there is a possibility to distinguish them from the light polarization dependence⁴⁵, because the Higgs modes are isotropic excitations while light-induced density fluctuations are generally not. In addition, the lower-energy peak of the Higgs modes is broadened and weakened in the presence of strong interband interactions, while that of density fluctuations is irrelevant to the interband interaction. Therefore, a line-shape analysis of THG resonance may help one to decompose the origin of observed data.

Now, let us display in Fig.7 the amplitude of Eqs.(49, 54, 55) for $i = x$ and that of total $j^{(3)x}(t)$ for monochromatic CW illumination $A(-\infty < t < \infty) = A_0 \sin \Omega t$, i.e., $A^2(\omega) = \frac{\pi}{2} A_0^2 [2\delta(\omega) - \delta(\omega - 2\Omega) - \delta(\omega + 2\Omega)]$, for $\lambda_I = -0.19$ (a) and $\lambda_I = -0.03$ (b). For large λ_I , the total third-order current has two peaks at $\Omega = \Delta_\alpha, \Delta_\beta$ [panel (a), black curve], which mainly arise from density fluctuations [red curve]. The Leggett mode resonance is broadened and weakened [blue curve], so that it is obscured in the total third-order current. By contrast, for small λ_I , the total third-order current exhibits three peaks [panel (b), black curve]. While the two peaks at $\Omega = \Delta_\alpha, \Delta_\beta$ primarily stem from density fluctuations [red curve], the lowest-energy peak is due to the Leggett mode and located at $2\Omega = \omega_L$ [blue curve]. This peak shows an asymmetric structure because of interference

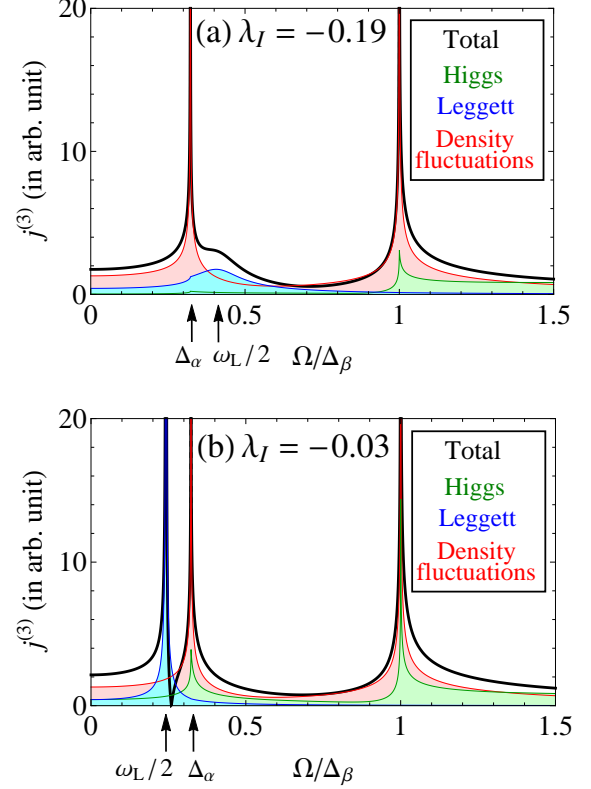


FIG. 7. Amplitudes of $j_H^{(3)x}$, $j_L^{(3)x}$, $j_d^{(3)x}$ and their sum $j^{(3)x}$ (green, blue, red and black curves, respectively) for $\lambda_I = -0.19$ (a) and -0.03 (b). Frequency Ω is normalized by the larger gap Δ_β . The positions of $\Omega = \Delta_\alpha$, $\omega_L/2$ are marked by arrows. Used parameters are $\lambda_{\alpha\alpha} = -0.28$, $\lambda_{\beta\beta} = -0.96$, $D_\alpha = 1$, $D_\beta = 0.73$, $\Delta_\alpha/\Delta_\beta = 0.31/0.96$, $c_{\alpha 0} = 0.5$, $c_{\beta 0} = -0.5$, $c_{\alpha 1} = c_{\beta 1} = -1$, $\tilde{c}_{\alpha 0} = \tilde{c}_{\beta 0} = 1$, $T = 0$.

between $j_L^{(3)}(t)$ and $j_d^{(3)}(t)$. We can then conclude that the Leggett mode can be detectable in a THG experiment when the interband Josephson coupling is so weak that $\omega_L < 2\Delta_\alpha$, where this mode is stable. The Higgs mode contribution is small compared to density fluctuations [green curves in Fig.7], independently of the value of λ_I within the mean-field theory.

VII. CONCLUSION

We have investigated collective modes excited resonantly by electromagnetic waves for two-band superconductors having different BCS gap energies. For weaker interband pairing interactions, there emerge three collective modes that can be optically excited: two Higgs modes corresponding respectively to amplitude oscillation of two components of the order parameter, and the Leggett mode corresponding to oscillation of the relative phase. For stronger interband interactions, which should include the case of MgB_2 , the Leggett mode and

one of the Higgs modes are destabilized with their resonances weakened. At finite temperatures, the Leggett mode slightly recovers its stability, while the Higgs mode associated with the smaller gap disappears; the Higgs mode with the larger energy always remains long-lived. We further find that all of these collective modes contribute to the third-harmonic generation (THG). Specifically, we have shown that the Leggett mode can be observable in THG experiments when it is stable. Density fluctuations also contribute to THG and have the same resonance frequency as the Higgs modes. However, THG from the lower-energy Higgs mode is weakened due to interband interaction while the lower-energy peak of THG from density fluctuations is not. Such a difference and polarization dependence may help one to experimentally distinguish the contributions from the Higgs modes and from density fluctuations.

Processes beyond the mean-field approximation, such as fluctuations and dynamical interaction, may affect the mode properties and nonlinear response. An even more interesting possibility is the interaction between the Leggett and the Higgs modes. When we consider higher-order processes beyond the linearized equation of motion, a coupling between these collective modes should appear, which is expected to lead to further features in the dynamical behavior of the order parameters. While we have concentrated on the linear regime here, the nonlinear couplings between coexisting collective modes will serve as an intriguing future problem.

An experimental observation of the Leggett and Higgs modes will provide a novel avenue for probing the interacting condensates in multiband superconductors. In the case of MgB₂, a terahertz wave will be suited for optically-resonant excitations, because superconductivity in this material has a similar energy scale to that in the recently reported single-band case¹⁸. Probing in terms of the collective modes may also be possibly applicable to the iron pnictides which are also multiband superconductors with a similar energy scale. In a broader context, the present analysis of collective modes is expected to pave a new pathway for obtaining information on pairing interactions, both intraband and interband, and a possibility of controlling superconductivity.

ACKNOWLEDGMENTS

We wish to thank A. J. Leggett for a valuable comment. We are also benefitted from discussions with R. Shimano, R. Matsunaga and K. Tomita. Discussions with K. Kuroki, M. Yamada, and A. Sugioka are also gratefully acknowledged. The present work was supported by Grants-in-Aid for Scientific Research from MEXT (Grant No. 26247057) and ImPACT project

(No. 2015-PM12-05-01) from JST. N.T. is supported by Grants-in-Aid for Scientific Research from JSPS (Nos. 25104709 and 25800192).

APPENDIX: TABLE OF SYMBOLS

In this appendix, we summarize the symbols used in the main text of the paper.

Symbol	Definition
$\gamma = \alpha \text{ or } \beta$	band indices; annihilation operators
Δ_γ	superconducting gaps [Eq.(3)]
$\lambda_{\gamma\gamma'}$	dimensionless paring interaction [Eq.(23)]
λ_I	dimensionless interband coupling [Eq.(38)]
$\det \lambda$	$\lambda_{\alpha\alpha}\lambda_{\beta\beta} - \lambda_{\alpha\beta}\lambda_{\beta\alpha}$ [Eq.(23)]
$\sigma_{\gamma\mathbf{k}}$	Anderson's pseudospin [Eq.(6)]
Ω	frequency of incident light
ω_c	cut-off energy in BCS gap equation
ω_{H_γ}	energy of Higgs modes: peak position of $ H_\gamma(\omega) $, equal to $2\Delta_\gamma$ [Sec. IV]
ω_L	energy of Leggett mode: peak position of $ L(\omega) $ [Sec. III]
$A^2(\omega)$	Fourier transform of squared vector potential $A(t)^2$
$\mathbf{b}_{\gamma\mathbf{k}}$	pseudomagnetic field [Eq.(8)]
$c_{\gamma 0}, c_{\gamma 1}$	expansion coefficients of $\sum_{\mathbf{k}} \delta(\epsilon - \epsilon_{\gamma\mathbf{k}}) \frac{\partial^2 \epsilon_{\gamma\mathbf{k}}}{\partial k_x^2}$ [Eq.(28)]
$c_{\gamma 0}^i$	expansion coefficient of $\sum_{\mathbf{k}} \delta(\epsilon - \epsilon_{\gamma\mathbf{k}}) \frac{\partial^2 \epsilon_{\gamma\mathbf{k}}}{\partial k_i \partial k_x}$ [Eq.(50)]
$\tilde{c}_{\gamma 0}^i$	expansion coefficient of $\sum_{\mathbf{k}} \delta(\epsilon - \epsilon_{\gamma\mathbf{k}}) \frac{\partial^2 \epsilon_{\gamma\mathbf{k}}}{\partial k_i \partial k_x} \frac{\partial^2 \epsilon_{\gamma\mathbf{k}}}{\partial k_x^2}$ [Eq.(53)]
D_γ	density of states on Fermi surface [Eq.(24)]
$E_{\gamma\mathbf{k}}$	Bogoliubov quasi-particle's energy [Eq.(14)]
$F_\gamma(\omega)$	Eq.(21) or (26): resonance factor for density fluctuations
$G_\gamma(\omega)$	Eq.(42): $(4\Delta_\gamma^2 - \omega^2)F_\gamma(\omega)$
$H_\gamma(\omega)$	Eq.(41): resonance factor for Higgs modes
$L(\omega)$	Eq.(30): resonance factor for Leggett mode
$V_{\gamma\gamma'}$	paring interaction [Eq.(1)]
$\det V$	$V_{\alpha\alpha}V_{\beta\beta} - V_{\alpha\beta}V_{\beta\alpha}$
$X_\gamma(\omega)$	Eq.(43): describes nonlinear coupling between light and Higgs modes
$Y_\gamma(\omega)$	Eq.(22) or (27): describes nonlinear coupling between light and Leggett mode

- ¹ Y. Nambu, Phys. Rev. **117**, 648 (1960).
- ² J. Goldstone, Nuovo Cimento **19**, 154 (1961).
- ³ J. Goldstone, A. Salam and S. Weinberg, Phys. Rev. **127**, 965 (1962).
- ⁴ P. W. Anderson, Phys. Rev. **130**, 439 (1963).
- ⁵ P. W. Higgs, Phys. Lett. **12**, 132 (1964).
- ⁶ F. Englert and R. Brout, Phys. Rev. Lett. **13**, 321 (1964).
- ⁷ P. W. Higgs, Phys. Rev. Lett. **13**, 508 (1964).
- ⁸ G. S. Guralnik, C. R. Hagen and T. W. B. Kibble, Phys. Rev. Lett. **13**, 585 (1964).
- ⁹ R. V. Carlson and A. M. Goldman, Phys. Rev. Lett. **34**, 11 (1975).
- ¹⁰ Y. Ohashi and S. Takada, J. Phys. Soc. Jpn. **66**, 2437 (1997). See also S. N. Artemenko and A. F. Volkov, <http://arxiv.org/abs/cond-mat/9712086>.
- ¹¹ A. F. Volkov and S. M. Kogan, Zh. Eksp. Teor. Fiz. **65**, 2038 (1973) [Sov. Phys. JETP **38**, 1018 (1974)].
- ¹² C. M. Varma, J. Low Temp. Phys. **126**, 901 (2002).
- ¹³ D. Pekker and C. M. Varma, Annu. Rev. Condens. Matter Phys. **6**, 269 (2015).
- ¹⁴ R. Sooryakumar and M. V. Klein, Phys. Rev. Lett. **45**, 660 (1980).
- ¹⁵ P. B. Littlewood and C. M. Varma, Phys. Rev. Lett. **47**, 811 (1981).
- ¹⁶ M.-A. Méasson, Y. Gallais, M. Cazayous, B. Clair, P. Rodière, L. Cario and A. Sacuto, Phys. Rev. B **89**, 060503(R) (2014).
- ¹⁷ R. Matsunaga, Y. I. Hamada, K. Makise, Y. Uzawa, H. Terai, Z. Wang and R. Shimano, Phys. Rev. Lett. **111**, 057002 (2013).
- ¹⁸ R. Matsunaga, N. Tsuji, H. Fujita, A. Sugioka, K. Makise, Y. Uzawa, H. Terai, Z. Wang, H. Aoki and R. Shimano, Science **345**, 1145 (2014).
- ¹⁹ N. Tsuji and H. Aoki, Phys. Rev. B **92**, 064508 (2015).
- ²⁰ P. Wölffe, Physica B **90**, 96 (1977).
- ²¹ Y. Barlas and C. M. Varma, Phys. Rev. B **87**, 054503 (2013).
- ²² A. J. Leggett, Prog. Theor. Phys. **36**, 901 (1966).
- ²³ S. G. Sharapov, V. P. Gusynin and H. Beck, Eur. Phys. J. B **30**, 45 (2002).
- ²⁴ F. J. Burnell, J. Hu, M. M. Parish and B. A. Bernevig, Phys. Rev. B **82**, 144506 (2010).
- ²⁵ Y. Ota, M. Machida, T. Koyama and H. Aoki, Phys. Rev. B **83**, 060507(R) (2011).
- ²⁶ S.-Z. Lin and X. Hu, Phys. Rev. Lett. **108**, 177005 (2012).
- ²⁷ N. Bittner, D. Einzel, L. Klam and D. Manske, Phys. Rev. Lett. **115**, 227002 (2015).
- ²⁸ P. Szabó, P. Samuely, J. Kačmarčík, T. Klein, J. Marcus, D. Fruchart, S. Miraglia, C. Marcenat and A. G. M. Jansen, Phys. Rev. Lett. **87**, 137005 (2001).
- ²⁹ M. Iavarone, G. Karapetrov, A. E. Koshelev, W. K. Kwok, G. W. Crabtree, D. G. Hinks, W. N. Kang, E.-M. Choi, H. J. Kim, H.-J. Kim and S. I. Lee, Phys. Rev. Lett. **89**, 187002 (2002).
- ³⁰ J. Kortus, I. I. Mazin, K. D. Belashchenko, V. P. Antropov and L. L. Boyer, Phys. Rev. Lett. **86**, 4656 (2001).
- ³¹ A. Y. Liu, I. I. Mazin and J. Kortus, Phys. Rev. Lett. **87**, 087005 (2001).
- ³² S. Souma, Y. Machida, T. Sato, T. Takahashi, H. Matsui, S.-C. Wang, H. Ding, A. Kaminski, J. C. Campuzano, S. Sasaki and K. Kadowaki, Nature **423**, 65 (2003).
- ³³ A. Brinkman, S. H. W. van der Ploeg, A. A. Golubov, H. Rogalla, T. H. Kim and J.S. Moodera, J. Phys. Chem. Solids **67**, 407 (2006).
- ³⁴ G. Blumberg, A. Mialitsin, B. S. Dennis, M. V. Klein, N. D. Zhigadlo and J. Karpinski, Phys. Rev. Lett. **99**, 227002 (2007).
- ³⁵ M. V. Klein, Phys. Rev. B **82**, 014507 (2010).
- ³⁶ D. Mou, R. Jiang, V. Taufour, R. Flint, S. L. Bud'ko, P. C. Canfield, J. S. Wen, Z. J. Xu, G. Gu and A. Kaminski, Phys. Rev. B **91**, 140502(R) (2015).
- ³⁷ K. Kuroki, S. Onari, R. Arita, H. Usui, Y. Tanaka, H. Kontani and H. Aoki, Phys. Rev. Lett. **101**, 087004 (2008).
- ³⁸ I. I. Mazin, D. J. Singh, M. D. Johannes and M. H. Du, Phys. Rev. Lett. **101**, 057003 (2008).
- ³⁹ K. Kuroki, H. Usui, S. Onari, R. Arita and H. Aoki, Phys. Rev. B **79**, 224511 (2009).
- ⁴⁰ T. Shibauchi, A. Carrington and Y. Matsuda, Annu. Rev. Condens. Matter Phys. **5**, 113 (2014).
- ⁴¹ S. Maiti and P. J. Hirschfeld, Phys. Rev. B **92**, 094506 (2015).
- ⁴² A. Moor, A. F. Volkov and K. B. Efetov, Phys. Rev. B **88**, 224513 (2013).
- ⁴³ M. Dzero, M. Khodas and A. Levchenko, Phys. Rev. B **91**, 214505 (2015).
- ⁴⁴ A. Moor, P. A. Volkov, A. F. Volkov and K. B. Efetov, Phys. Rev. B **90**, 024511 (2014).
- ⁴⁵ T. Cea, C. Castellani and L. Benfatto, Phys. Rev. B **93**, 180507(R) (2016).
- ⁴⁶ P. W. Anderson, Phys. Rev. **112**, 1900 (1958).
- ⁴⁷ The Higgs mode contribution Eq.(49) is not modified by screening in our model, where k -independent gap functions and constant density of states around the Fermi energy are assumed.